Article

Prediction of Delamination Defects in Drilling of Carbon Fiber Reinforced Polymers Using a Regression-Based Approach

Mohammad Ghasemian Fard [1], Hamid Baseri [1], Aref Azami [2,*] and Abbas Zolfaghari [1]

[1] Department of Mechanical Engineering, Babol Noshirvani University of Technology, Babol 47148-71167, Iran; m.ghasemian3058@gmail.com (M.G.F.); h.baseri@nit.ac.ir (H.B.); zolfaghari@nit.ac.ir (A.Z.)

[2] Center for Precision Engineering, Department of Design, Manufacturing & Engineering Management, University of Strathclyde, Glasgow G1 1XQ, UK

* Correspondence: aref.azamigilan@strath.ac.uk

Abstract: Carbon fiber-reinforced polymer (CFRP) structures have been increasingly used in various aerospace sectors due to their outstanding mechanical properties in recent years. However, the poor machinability of CFRP plates, combined with the inhomogeneous behavior of fibers, poses a challenge for manufacturers and researchers to define the critical factors and conditions necessary to ensure the quality of holes in CFRP structures. This study aims to analyze the effect of drilling parameters on CFRP delamination and to predict hole quality using a regression-based approach. The design of the experiment (DOE) was conducted using Taguchi's L9 3-level orthogonal array. The input drilling variables included the feed rate, spindle speed, and three different drill types. A regression-based model using partial least squares (PLS) was developed to predict delamination defects during the drilling of CFRP plates. The PLS model demonstrated high accuracy in predicting delamination defects, with a Mean Squared Error (MSE) of 0.0045, corresponding to an accuracy of approximately 99.6%, enabling the rapid estimation of delamination. The model's predictions were closely aligned with the experimental results, although some deviations were observed due to tool inefficiencies, particularly with end mill cutters. These findings offer valuable insights for researchers and practitioners, enhancing the understanding of delamination in CFRPs and identifying areas for further investigation.

Keywords: CFRPs; delamination; drilling; PLS regression

1. Introduction

Carbon fiber-reinforced polymers (CFRPs) are extensively utilized in the aerospace and automotive industries due to their exceptional strength-to-weight ratio and fatigue resistance. Delamination, a critical defect often induced during the drilling of CFRP composites, significantly compromises structural integrity. This damage mechanism, characterized by the separation of composite layers, adversely impacts long-term performance and precision assembly. The heterogeneous and anisotropic nature of composite materials can predispose the region surrounding a drilled hole to damage. Delamination, fiber pullout, interlaminar cracking, and thermal damage constitute the primary defects arising from the drilling of CFRPs composites [1]. These defects account for approximately 60% of production rejects due to drilling, significantly compromising long-term structural integrity and dimensional accuracy [2]. Drilling, a critical machining operation for composite components, particularly CFRP laminates, often results in delamination, compromising structural integrity. The generation of substantial thrust forces, especially at the entry and exit points of a drill, is the primary factor contributing to this damage mechanism. These forces can exceed the interlaminar bond strength, leading to delamination and the subsequent degradation of the composite load-bearing capacity and dimensional stability [3]. Numerous problems arise as a result of less-than-optimal cutting edges, rapid tool wear, and drilling situations [4,5]. The intricate interaction between the drill bit's cutting edges and the CFRP

workpiece significantly influences the formation of internal hole defects. This dynamic interplay is the primary determinant of the final hole quality, with implications for the overall structural integrity of the composite component [6,7]. Delamination in CFRP drilling is intricately linked to the cutting speed, drill size, and feed rate, forming a complex interplay of variables. Comprehensive experimental investigations are required to elucidate these relationships. To gain deeper insights into the underlying mechanisms, researchers have employed a combination of experimental and computational methodologies. Statistical tools, including ANOVA and Taguchi methods, have been instrumental in developing empirical models for CFRP drilling processes. Davim and Reis [8] investigated how the cutting speed and feed rate are related to delamination in a composite plate using Taguchi's method and ANOVA. Tsao and Hocheng [9] used a twist drill and two types of core drills to predict and evaluate the delamination factor. Due to the complexity of machining processes, these methods need a lot of input machining parameters and computational resources. Experiments with a lot of variables and a small number of experiments are often designed using the Taguchi orthogonal array [10]. It should be noted that the Taguchi method minimizes unmanageable variables, which do not provide a numerical correlation between variables and target results. In recent years, there has been increasing interest in modeling significant physical parameters and materials performance based on data-driven approaches [11–13]. In order to investigate the connection between machining variables and efficiency, researchers combine experimental design methods with statistical methods [14]. Methods like these are typically classified as regression-based approaches that are capable of handling a certain level of uncertainty, imprecision, and approximation. Through the utilization of machine learning techniques, it has become possible to accurately forecast and identify crucial machining parameters. For predicting surface roughness in face milling, three models have been developed: regression analysis, Bayesian neural networks, and support vector machines [15]. The prediction of machining forces has also been made possible through a number of neural network-based methods. For modeling the cutting forces during end milling with a high-speed steel tool and aluminum material, a multilayer perceptron network was developed [16]. The cutting force during face milling was predicted by an artificial neural network (ANN). There are three types of descriptive parameters, spindle speed, the feed rate, and the depth of cut, and with a 10% error margin, the model can estimate the cutting force [17]. The main features used to compare models are the average percentage error, the generalization ability, and run time. Nevertheless, these modeling approaches have room for improvement.

The use of appropriate drilling parameters is crucial to avoid delamination and ensure the quality of the hole. In recent years, statistical modeling has gained popularity in predicting the quality of the hole and delamination in CFRP drilling. The purpose of this study is to analyze the effect of drilling parameters on CFRP delamination and hole quality prediction using a regression-based approach. Partial least squares (PLS) models are probabilistic models and require a modest amount of time to run. There is no information yet on the possibility of this method's prediction of CFRP delamination during drilling. We selected drilling tools based on their distinct mechanisms and high efficiency in generating hole quality and minimizing machining forces, aligning with our primary goal of analyzing drilling parameters' effects on CFRP delamination and hole quality prediction. A PLS model is developed in this study to predict the delamination factor for CFRP laminates as a result of spindle speed, different tool geometries, and the feed rate in different machining environments (wet and dry). Also, the Taguchi method is used for the design of experiments.

2. Test Methodology and Specimen Preparation

Table 1 presents the mechanical properties of the CFRP plates fabricated for this study employing the hand lay-up technique, employing carbon fiber-woven fabrics as reinforcement and an epoxy resin matrix (Epon-828) with a density of 1.16 g/mL and equivalent weight of 185–192 g/eq. The high tensile strength (3800 MPa) of the carbon

fibers provides excellent durability during the drilling process, while a Young's modulus of 62 GPa ensures the structural integrity of the CFRP plates under mechanical stress. These properties were critical in minimizing deformation and maintaining stability during the tests [18]. The woven fabric was selected to enhance the in-plane mechanical properties and provide a quasi-isotropic structure by the fiber orientation [0° and 90°] across layers. Each composite layer was 0.2 mm thick, ensuring uniformity and stability in the final structure. A rectangular stack workpiece with a length of 17 cm, a width of 10 cm, and a thickness of 7 mm was used. After completing the drilling operation and analyzing the delamination defects at the entry hole, the specimens were cut to facilitate the optical microscopy analysis of the internal structure. This preparation step involved precisely sectioning the drilled holes to ensure a clear view of the internal features. The optical microscope was utilized to capture images of the cross-sections; however, the resolution limitations of this method may hinder the accurate visualization of subtle internal defects. Therefore, it is recommended that further investigations using scanning electron microscopy (SEM) be conducted to achieve a more detailed examination of the internal structure and to effectively characterize any defects present.

Table 1. Mechanical properties of CFRP plates.

Parameters	Units
Tensile strength (GPa)	3800
Young modulus (GPa)	62
Shear strength (MPa)	75
Glass transition (°C)	170

Table 2 outlines the details of the experiments. To achieve reliable results, three ranges of feed rates and spindle speeds were selected to meet CFRP drilling requirements. The JOHNFORD VMC 600 three-axis vertical milling machine with a spindle drive of 5.5 kW was used for the drilling tests (Figure 1). Also, a Mitutoyo TM-500 microscope was used to measure damage around the holes. As shown in Figure 2, the drilling experiments were conducted on CFRP plates using three drills with 6 mm diameters. Drill types A, B, and C were employed for this study, comprising a solid carbide drill with internal cooling channels (a), a cobalt end mill (b), and a two-step drill (c), respectively. The choice of an end mill cutter enables us to explore how its geometry affects the cutting dynamics in composite materials, particularly in terms of delamination defect generation. This exploration is crucial, as it not only sheds light on the practical implications of using non-dedicated tools for drilling but also emphasizes the need for a comprehensive understanding of tool interactions with composite structures. Our findings aim to inform future tool selection and design considerations in the machining of advanced materials. By contrasting the performance of tools under both cooled (Tool (a)) and dry conditions (Tools (b) and (c)), the study aims to deepen the understanding of how these variables influence delamination in carbon fiber composites, ultimately guiding future tool selection and machining strategies.

Table 2. Drilling operation input variables.

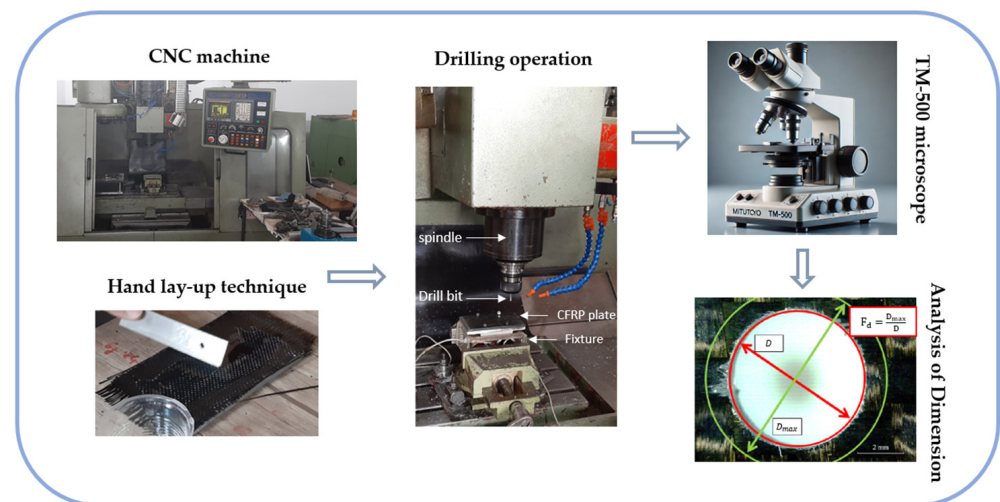| Level	Spindle Speed (RPM)	Feed Rate (mm/rev)	Tool
1	1000	0.02	(a)
2	2000	0.05	(b)
3	3000	0.79	(c)

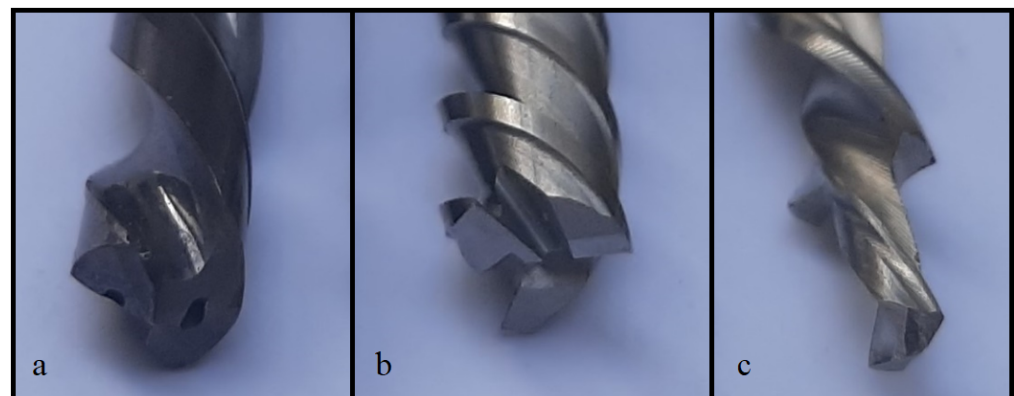**Figure 1.** Experimental set-up of CFRP plate drilling.

Figure 2. Three types of drills used: (**a**) solid carbide drill, (**b**) cobalt end mill, and (**c**) step drill.

3. Taguchi Method

The Taguchi method was used for the design of the experiment and optimize the process parameters. Table 3 outlines the experimental input parameters and levels used in the drilling trials, as well as the results of the analysis of drilled holes, specifically the delamination factor (F_d). The L27 orthogonal array was selected for its efficacy in identifying factor interactions. Delamination factor prediction was used as a quality character factor for optimizing machining variables like the spindle speed (A), feed rate (B), and tool structure (C). To assess the influence of various factors on CFRP laminate delamination, both mean values and signal-to-noise (S/N) ratios were calculated. Given the objective of minimizing delamination, a 'smaller is better' S/N ratio approach was adopted, as expressed by the following equation:

Lower is the best:

$$\frac{S}{N} = -10 \log \frac{1}{n} \sum\nolimits_{i=1}^{n} y_i^2 \tag{1}$$

The experimental data (i) are averaged out of (n) repeated experiments, and (y_i) represents the average measured value.

Table 3. Sequence of data and predictions based on Taguchi method.

Test No.	Factors			Condition	Delamination (F_d)	PLS Prediction	S/N Ratio
	A	**B**	**C**				
1	1000	0.02	1	$A_1B_1C_1$	1.014	1.018	−0.12076
2	1000	0.05	1	$A_1B_2C_1$	1.043	1.018	−0.36569
3	1000	0.79	1	$A_1B_3C_1$	1.031	1.026	−0.26517
4	2000	0.02	1	$A_2B_1C_1$	1.035	1.055	−0.29881
5	2000	0.05	1	$A_2B_2C_1$	1.032	1.056	−0.27359
6	2000	0.79	1	$A_2B_3C_1$	1.025	1.063	−0.21448
7	3000	0.02	1	$A_3B_1C_1$	1.024	1.093	−0.206
8	3000	0.05	1	$A_3B_2C_1$	1.028	1.094	−0.23986
9	3000	0.79	1	$A_3B_3C_1$	1.027	1.101	−0.23141
10	1000	0.02	2	$A_1B_1C_2$	1.061	1.061	−0.51431
11	1000	0.05	2	$A_1B_2C_2$	1.063	1.061	−0.53067
12	1000	0.79	2	$A_1B_3C_2$	1.098	1.069	−0.81205
13	2000	0.02	2	$A_2B_1C_2$	1.1	1.098	−0.82785
14	2000	0.05	2	$A_2B_2C_2$	1.287	1.099	−2.19157
15	2000	0.79	2	$A_2B_3C_2$	1.217	1.107	−1.70581
16	3000	0.02	2	$A_3B_1C_2$	1.102	1.136	−0.84363
17	3000	0.05	2	$A_3B_2C_2$	1.271	1.137	−2.08291
18	3000	0.79	2	$A_3B_3C_2$	1.285	1.144	−2.17806
19	1000	0.02	3	$A_1B_1C_3$	1.063	1.104	−0.53067
20	1000	0.05	3	$A_1B_2C_3$	1.065	1.104	−0.54699
21	1000	0.79	3	$A_1B_3C_3$	1.093	1.112	−0.7724
22	2000	0.02	3	$A_2B_1C_3$	1.063	1.142	−0.53067
23	2000	0.05	3	$A_2B_2C_3$	1.109	1.142	−0.89863
24	2000	0.79	3	$A_2B_3C_3$	1.137	1.150	−1.11521
25	3000	0.02	3	$A_3B_1C_3$	1.113	1.179	−0.9299
26	3000	0.05	3	$A_3B_2C_3$	1.162	1.180	−1.30412
27	3000	0.79	3	$A_3B_3C_3$	1.2	1.187	−1.58362

4. Partial Least Squares (PLS) Regression for Multivariate Performance Analysis

To control collinearity among the variables, the data were transformed into a lower-dimensional space using partial least squares regression (PLSR), identifying a linear regression model [19]. PLS regression is a statistical method that combines features from principal component analysis (PCA) and multiple regression. It is particularly useful when predictor variables are highly collinear or when the number of predictors exceeds the number of observations. The PLS regression finds the fundamental relations between two matrices (predictor matrix X and response matrix Y), aiming to predict Y from X and describe their common structure. The relationship between two groups of variables, X (predictors) and Y (responses), is extensively studied within the formulated new space. The PLS regression is a supervised learning model used for both regression and classification problems. It falls under the category of linear regression techniques, but it addresses the limitations of ordinary least squares (OLS) regression when predictors are highly collinear or when there are more predictors than observations. PLS regression seeks to project predictor variables X and response variables Y into a new space where they are maximally correlated. The key steps involved in PLS regression include constructing new latent variables (components) as linear combinations of the original predictor variables, choosing components that capture the maximum covariance between the predictors and the responses, and regressing the response variables on the latent variables rather than on the original predictor variables. This process involves a thorough analysis of the data in both spaces. By isolating the direction in the X space that explains the variation in the Y space, the model can make better predictions and understand the relationships between the two spaces. This method's primary goal is to

determine the underlying factors of the most significant degree of variation. In PLSR, the variance between predictors and responses can be expressed mathematically as follows:

$$X = TP^T + E \qquad (2)$$

$$Y = UQ^T + F \qquad (3)$$

Here, matrices X and Y represent the predictors (an n × m matrix) and responses (an n × p matrix), respectively. Matrices T and U have dimensions n × l, representing projections of scores for X and Y. Matrices P and Q define the perpendicular direction of the X and Y scores that have been projected. The predictor matrix and the response matrix both have error terms labeled E and F, assumed to be unrelated to each other.

The primary goal of this study is to utilize the underlying factors to make predictions about the responses within the population. Obtaining factors T and U (the projection of the X and Y scores from a data set), the latent variables using both X (predictors) and Y (responses) values were extracted. The number of factors extracted was determined based on the amount of variance that can be accounted for with the least possible number of factors. This means finding the most efficient way to explain the variance in the data so that the fewest number of factors can explain the most variance. This ensures that the factors extracted are relevant to the data and capture the most meaningful information. The 'plsregress' feature was employed using MATLAB version 2019b to implement the partial least squares (PLS) regression model. The PLS regression algorithm can be summarized by the following steps and equations:

The standardization of the predictor and response variables is essential to ensure that they are on a comparable scale and have a mean of zero and a standard deviation of one. This step is expressed as follows:

$$X_{sdt} = X - \frac{1}{n}\sum_{i=1}^{n} X_i D_X^{-1} \qquad (4)$$

$$Y_{sdt} = Y - \frac{1}{n}\sum_{i=1}^{n} Y_i D_Y^{-1} \qquad (5)$$

Here, X and Y represent the original predictor and response matrices, respectively. D_X and D_Y are diagonal matrices containing the standard deviations of the columns of X and Y. This step ensures that each variable has a mean of zero and a standard deviation of one, which is crucial for the stability and interpretability of the model.

The initialization step involves setting the initial values of the standardized predictor and response matrices. This sets the stage for the iterative extraction of components:

$$X_0 = X_{sdt} \qquad (6)$$

$$Y_0 = Y_{sdt} \qquad (7)$$

For each component k (from 1 to the desired number of components), the following steps are performed:

The weights are computed as the eigenvector corresponding to the largest eigenvalue of the matrix product $\left(X_{K-1}^T Y_{K-1}\right)\left(Y_{K-1}^T X_{K-1}\right)$:

$$W_k = \arg \max_{\|W\|=1} W^T \left(X_{K-1}^T Y_{K-1} Y_{K-1}^T X_{K-1}\right) W \qquad (8)$$

This step identifies the direction in the predictor space that maximizes the covariance with the response variables. The weights (W_k) serve as a bridge between the predictors and the responses, helping to extract meaningful components.

The latent variable or score t_k is computed by projecting the standardized predictor matrix X_{K-1} onto the weights (W_K):

$$t_k = X_{K-1}W_K \tag{9}$$

The score (t_k) represents the new latent variable that captures the most significant variation in the predictors in the direction defined by (W_K).

The score vector t_k is normalized to have a unit length to ensure that the scale of the components remains consistent:

$$t_k = \frac{t_k}{\| t_k \|} \tag{10}$$

Normalizing (t_k) ensures that the extracted components are comparable across different iterations.

The loadings for the predictor and response matrices are computed as follows:

$$p_k = \frac{X_{K-1}^T t_k}{t_K^T t_k} \tag{11}$$

$$q_k = \frac{Y_{K-1}^T t_k}{t_K^T t_k} \tag{12}$$

These equations compute the directions in the original spaces of *X* and *Y* that correspond to the latent variable (t_k). The loadings (p_k) and (q_k) provide insights into the relationships between the original variables and the extracted components.

The matrices *X* and *Y* are deflated to remove the effect of the extracted component. This ensures that the next component is orthogonal to the previous ones:

$$X_k = X_{k-1} - t_k p_k^T \tag{13}$$

$$Y_k = Y_{k-1} - t_k q_k^T \tag{14}$$

Deflating *X* and *Y* helps to isolate the unique information captured by each component, improving the overall interpretability of the model.

After extracting the desired number of components (say A), the regression model can be expressed as

$$Y_{sdt} = TQ^T + E \tag{15}$$

where $T = [t_1, t_2, \ldots, t_A]$ is the matrix of latent variables, and $Q = [q_1, q_2, \ldots, q_A]$ is the matrix of loading for *Y*. *E* represents the residual matrix. This equation represents the final relationship between the predictor and response matrices after extracting the components. It encapsulates the entire modeling process, capturing the essential relationships between predictors and responses.

For a new observation (X_{new}), the predicted response (Y_{new}) is given by

$$y_{new} = Y_{sdt} T^T \left(TT^T \right)^{-1} x_{new} \tag{16}$$

This equation allows for the prediction of new response values based on new predictor data using the previously obtained regression model. It provides a practical way to apply the PLS model to new data, ensuring that the extracted relationships are leveraged for prediction. The selection of latent variables in PLS regression involves criteria such as cross-validation techniques, explained variance, or other relevant metrics. The cumulative explained variance mathematically validates the effectiveness of our model in capturing underlying patterns. For robustness, the model underwent cross-validation to assess predictive performance, with the cross-validation error calculated through relevant equations, thereby adding credibility to the model's predictive capabilities. To enhance the comprehensibility of the PLS model, this study delved into the correlation between the

extracted latent variables and the underlying physical and mechanical characteristics of the carbon fiber composite during the drilling process. This involved additional equations or expressions that bridge the gap between abstract latent variables and real-world implications. A sensitivity analysis was performed to assess how changes in model parameters or input variables (the spindle speed, feed rate, and tool structures) in wet and dry machining environments influence predictions. The equations or expressions for sensitivity analysis demonstrate the stability and reliability of our model under different conditions.

5. PLS Implementation

The 'plsregress' function was employed using MATLAB with the following syntax:

$$[XL, YL, XS, YS, BETA, PCTVAR] = plsregress(X, Y, ncomp); \tag{17}$$

This function is pivotal in the PLS regression analysis used in this study, generating essential outputs that facilitate a thorough understanding of the model.

Predictor Scores, XS: These scores represent linear combinations of variables within matrix X. They capture the relationships between the predictor variables and enable a deeper exploration of their impact on the model.

Response Scores, YS: These scores are constructed by combining responses linearly with PLS components XS that exhibit strong relationships. These scores help elucidate the patterns in the response variables, aiding in the interpretation of the model's predictions.

Coefficient Estimates Matrix (BETA): The matrix BETA contains coefficient estimates for the PLS regression. Notably, to compute accurate coefficient estimates for a model that includes intercept terms, a column of ones must be added to matrix X, known as intercepts. The inclusion of intercepts is essential for calculating the model's intercept, representing the point at which the regression line crosses the y-axis. The numerical coefficient estimates for PLS regression are presented as a matrix of numeric values. Table 4 displays the estimated beta values derived from our study data. The formula for BETA is given by

$$\text{BETA is a } (p + 1)\text{–by–}m \text{ matrix} \tag{18}$$

Table 4. Beta values.

	1	2
1	0.0343	0.9370
2	0.2400	0.0105
3	0.3928×10^{-4}	3.7833×10^{-5}
4	0.9884	0.0431

In Equation (18), 'p' denotes the number of predictor variables, and 'm' denotes the number of response variables. The predictor variables are utilized to predict the response variables, and their relationship is expressed through a mathematical equation. The first row of the BETA matrix contains estimated coefficients for the intercept terms, capturing the overall trend in the data. The estimated coefficients provide insights into how each independent variable influences the dependent variable. Table 4 presents the estimated beta values derived from our study data.

PCTVAR (Percentage of Variance): PCTVAR is described as a percentage of variance explained by the regression model. This metric is crucial in understanding the overall explanatory power of the model. As part of the analysis of the predictors in X, a PLS regression analysis is conducted on 27 components of the responses in Y. Through this procedure, a line equation will be generated:

$$y = X \cdot \beta_{2:4,2} + \beta_{1,2} \tag{19}$$

This equation encapsulates the relationship between predictor variables and responses, providing a succinct representation of the predictive capabilities of our PLS regression model. Figure 3 presents the architecture of the PLS regression model, including spindle speed, feed rate, and tool number as input variables, transforming them into latent variables (LV1 to LV4) to predict delamination (Fd). The connections illustrate the relationships between input, latent, and output layers, with path coefficients representing the model's learned weights.
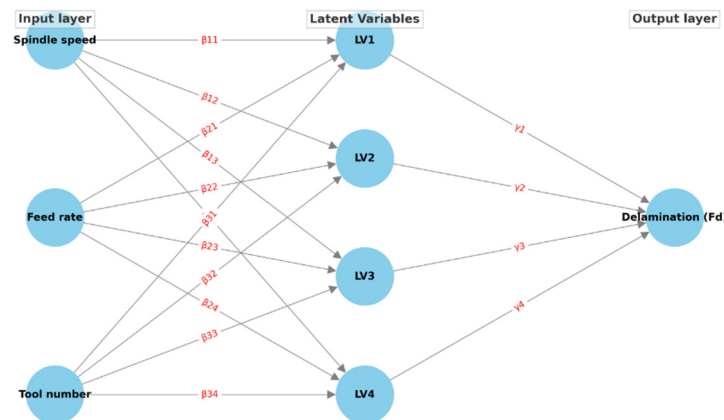
Figure 3. Detailed PLS regression model architecture.

6. Results and Discussion

6.1. Experimental Results

An essential consideration for improving the performance of composite components is the evaluation and monitoring of delamination factors that may occur during the drilling process. Therefore, a thorough understanding of delamination and its potential occurrence during drilling is crucial for ensuring the reliability and durability of composite structures. Composite delamination occurs when there is a separation between two adjacent layers, which significantly impacts the performance and fatigue life of composite plate assemblies [20]. In this study, the delamination factor $F_d = \frac{D_{max}}{D}$ was used, where Dmax represents the maximum diameter of the delaminated area, and D is the nominal diameter of the drilled hole. This formula provides a straightforward measure of the delamination extent by capturing the largest radial distance of damage around the hole. This approach is widely adopted in the literature due to its effectiveness in capturing the most significant radial damage [21]. Although alternative methods, such as calculating the delamination factor based on the ratio of delaminated area to hole area [22,23], provide additional detail, the maximum-diameter approach offers a reliable and straightforward metric that aligns with the objectives of this study. It allows us to observe trends in delamination without requiring extensive image processing. The microscope used in this study to measure damage around the holes is the Mitutoyo TM-500, manufactured by Mitutoyo Corporation (Kanagawa, Japan) and sourced from a distributor in China, as depicted in (Figure 4). After recording the maximum diameter (Dmax) around each hole in the damaged area, the value of the delamination factor (Fd) was determined. This factor is calculated by comparing the maximum diameter (Dmax) of a damage zone with the diameter (D) of the hole. The equation below can be used to compute the delamination factor (Fd):

$$F_d = \frac{D_{max}}{D} \tag{20}$$

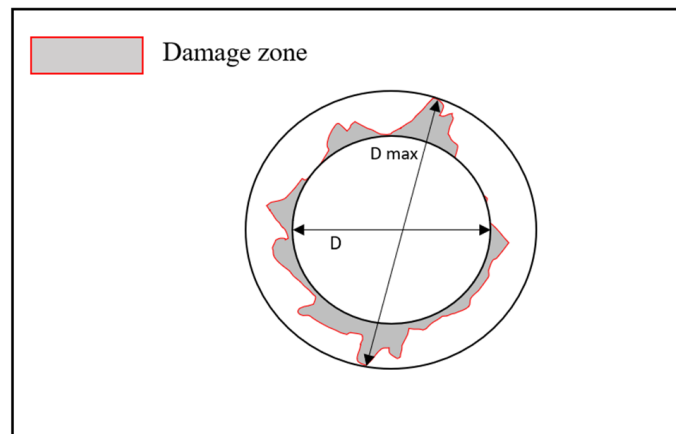A damaged hole has a maximum diameter of (Dmax) and a diameter of (D) in micrometers.

Figure 4. Measurement scheme for the maximum diameter of damages (Dmax).

Figure 5 shows that increasing the cutting speed up to 2000 rpm in drilling by Tool (a) and an interior cooling system, with feed rates of 0.05 and 0.79 mm/rev, resulted in a reduction in delamination. This reduction remained stable, even when the speed was further increased to 3000 rpm. Notably, a feed rate of 0.02 mm/rev consistently resulted in the lowest delamination across nearly all cutting speeds. Contrary to previous research, it appears that machining in a wet environment has a more positive impact, with cooling showing a significant influence, potentially even surpassing that of other input variables. Figure 6 illustrates a significant growth in delamination defects when the cutting speed is increased in drilling with Tool (b) cobalt end mill, using feed rates of 0.05 and 0.79 mm/rev. Conversely, lower defects were recorded using a 0.02 mm/rev in drilling operation, which remained constant across spindle speeds of 2000 rpm to 3000 rpm. From this trend, it was found that the feed rate in a dry drilling environment can have a more significant impact on machining results. Figure 7 displays similar mechanical behavior in drilling at feed rates of 0.05 and 0.79 using a step drill. Increasing the feed rate caused more delamination. The lowest delamination was observed at a feed rate of 0.02 around 1.065 (µm), and this value remained constant from 1000 rpm to 2000 rpm but increased at 3000 rpm. In general, delamination increased with feed rate in all cutting environments, which agreed with the findings of [24], and this was related to delamination damage formation mechanisms. From the recorded data, it can be understood that the fiber delamination generated by the Tool (a) and the cooling system has the lowest reaction value to the cutting variable. When the feed rate reached the maximum value of 0.79 mm/rev and the number of holes increased, the delamination coefficient produced by the step drill and milling tool worsened because the thrust force attained the top level in the composite plate. This phenomenon might be due to the geometrical difference between the two types of drills and the friction conditions. The drilling operation's thrust force often caused delamination damage, leading to interlaminar debonding between adjacent plies of a composite. This resulted in push-out delamination around the hole, with severity increasing as the thrust force increased. This phenomenon also explained why the trend of delamination regarding machining parameters in cooling conditions by Tool (a) was much lower than the results obtained in dry drilling conditions.
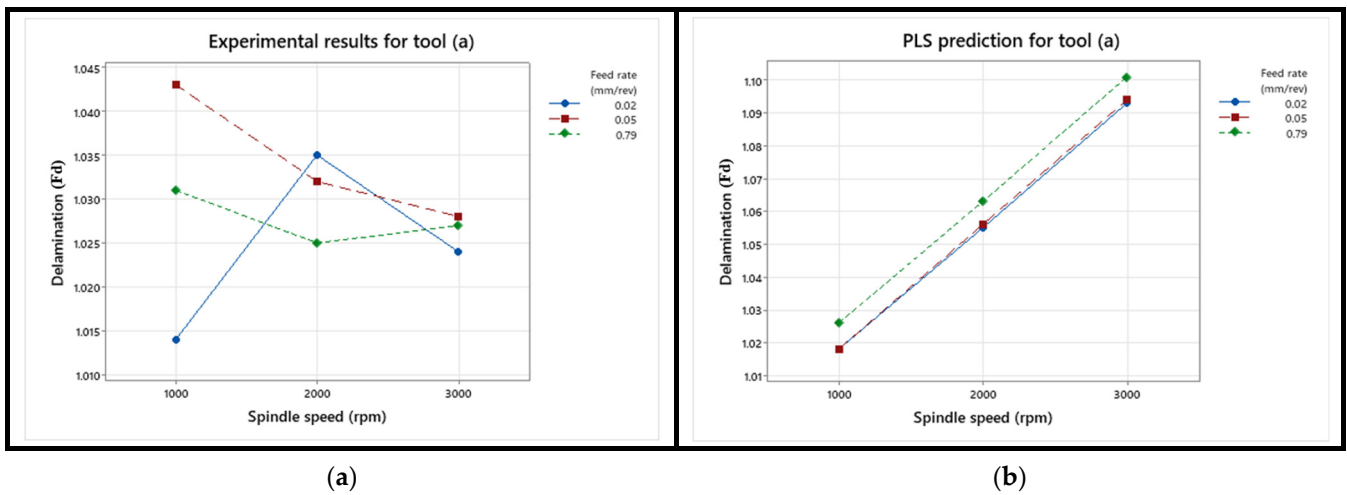
(**a**)　　　　　　　　　　　　　　　　　　(**b**)

Figure 5. Comparison between (**a**) experimental results and (**b**) PLS regression results for delamination defect made by solid carbide drill.
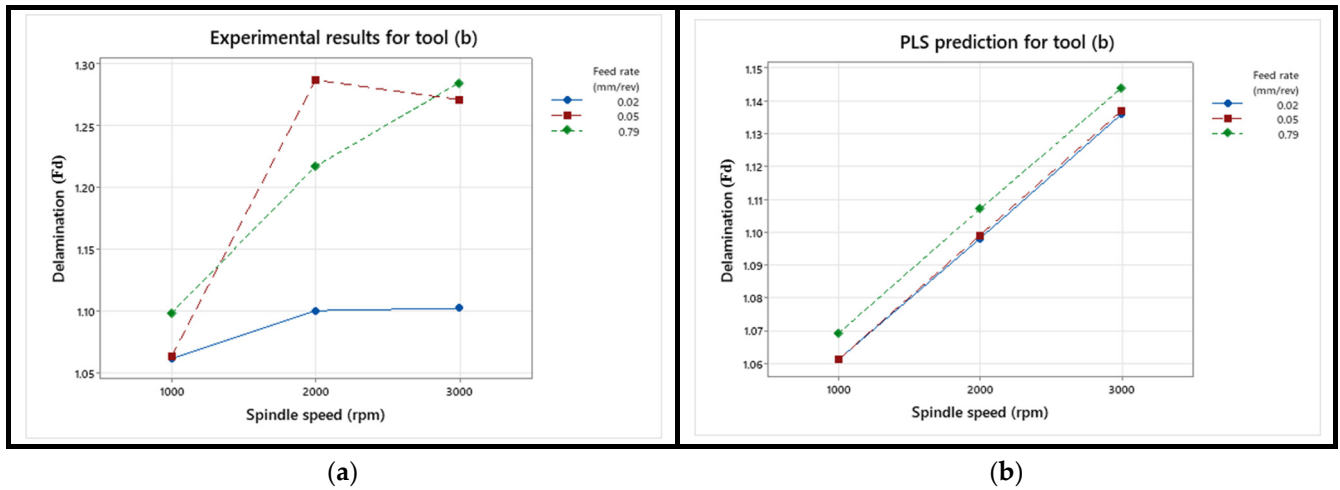

(**a**)　　　　　　　　　　　　　　　　　　(**b**)

Figure 6. Comparison between (**a**) experimental results and (**b**) PLS regression results for delamination defect made by cobalt end mill.
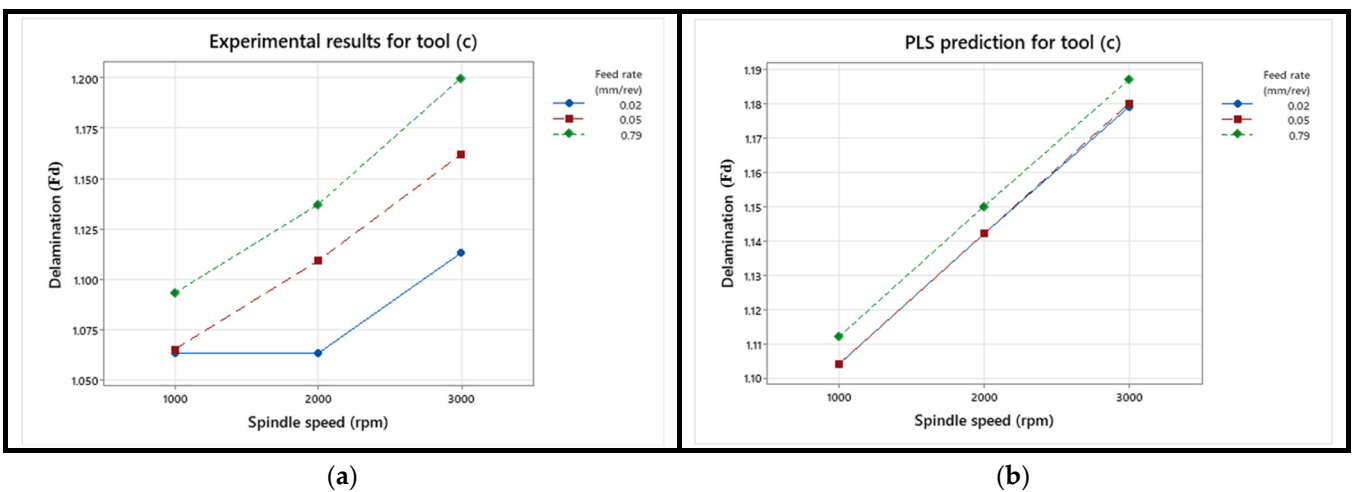

(**a**)　　　　　　　　　　　　　　　　　　(**b**)

Figure 7. Comparison between (**a**) experimental results and (**b**) PLS regression results for delamination defect made by step drill.

While delamination is typically assessed at the entry hole, examining the hole walls provides critical insights into the extent of internal damage and the overall quality of the drilled hole. The integrity of the hole walls is crucial for the structural performance of the composite, as defects here can propagate under load, leading to long-term failures [25]. While our focus has been on entrance delamination due to its critical impact on structural integrity and surface quality, we acknowledge that exit delamination also significantly affects mechanical properties. According to Tsao and Hocheng [26], defects at the exit point can significantly impact the performance of drilled components. Future studies will explore the role of exit delamination, particularly with milling cutters, for a more comprehensive understanding of delamination in composite machining. Figure 8 shows a visual comparison of delamination defects for Tools (a), (b), and (c). For Tool (a), the solid carbide drill with internal cooling channels, the lower delamination can be attributed to its optimized geometry and efficient heat dissipation, which helps maintain cutting stability and reduce thermal-induced damage. The cooling channels also aid in chip evacuation, further minimizing mechanical stress on the composite. For Tool (b) (end mill) and Tool (c) (two-step drill), both tools produced larger delamination defects than Tool (a), with Tool (b) showing the most pronounced damage. This could be due to the helical flutes of the end mill, which introduce higher lateral forces, leading to increased fiber pull-out and matrix cracking. Additionally, the lack of internal cooling in Tool (b) exacerbates heat accumulation and tool wear, further contributing to the defects. On the other hand, Tool (c), while also causing substantial damage, produced slightly smaller defects than Tool (b), likely owing to the step geometry. Although the two-step design creates additional cutting forces at the transition points, it may have distributed the forces in a way that mitigates some of the damage observed with Tool (b). However, both tools exhibited significant delamination compared to Tool (a), in line with the higher (Fd) values from the Taguchi analysis.
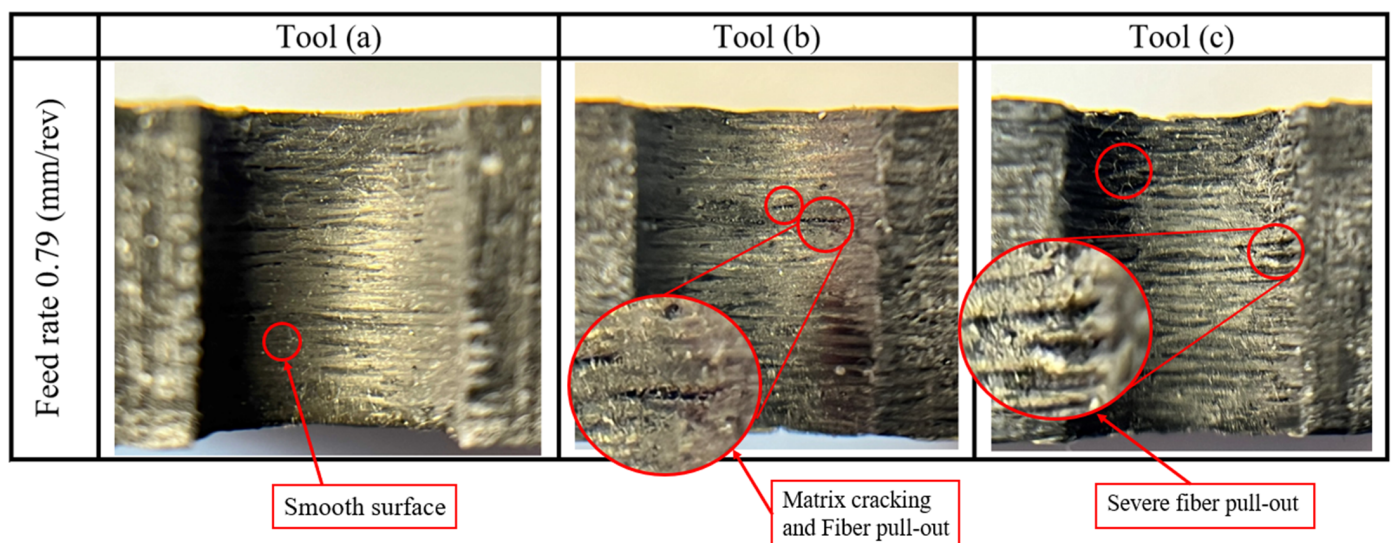

Figure 8. Visual comparison of delamination defects for Tool (**a**), Tool (**b**), and Tool (**c**) at 3000 RPM and 0.79 mm/rev feed rate.

6.2. PLS Regression Model Results

In this section, a comparative analysis between the experimental results and the predictions generated by the statistical model (PLS) is presented. The purpose of this comparison is to assess the accuracy and reliability of the model in predicting delamination defects in composite CFRP materials. The experimental data were collected under controlled conditions to ensure consistency across all samples. The input parameters of the network are the spindle speed, feed rate, and type of tools with different structures and its output parameters also include the delamination factor. Both datasets were processed to eliminate outliers and normalized to facilitate a direct comparison. As shown in Figure 9, the

model's predictions closely match the experimental results, especially during tests 1 to 6, which correspond to the holes drilled with Tool (a) at 1000 and 2000 rpm. However, some deviations were observed from test numbers 13 to 19, which could be attributed to end mill cutters being less efficient at removing chips compared to other tools like a step drill or a drill bit with the cooling system. This inefficiency can cause chips to clog the cutting path, especially as the number of drilling operations increases. This clogging may elevate the temperature in the cutting zone, leading to thermal damage to the CFRP material. The accumulation of heat could further exacerbate the deviations in performance over successive drilling operations. The regression-based approach developed for predicting delamination in CFRPs materials demonstrates impressive accuracy and stability, as evidenced by the statistical analysis of the prediction errors. Specifically, the model's performance was evaluated using the Mean Squared Error (MSE) metric, which provides a measure of the average squared difference between the predicted and actual values. The MSE for this model was calculated to be 0.0045, indicating a very low level of prediction error. This low MSE indicated minimal variance between the predicted and actual values, translating to an accuracy of approximately 99.6%. Such precision is crucial for applications requiring reliable predictions of delamination. Moreover, the model's consistent performance across different test cases underscores its robustness, making it a reliable tool for predicting delamination in CFRP components and supporting its potential for broader applications. These findings support the potential application of this model in manufacturing engineering.
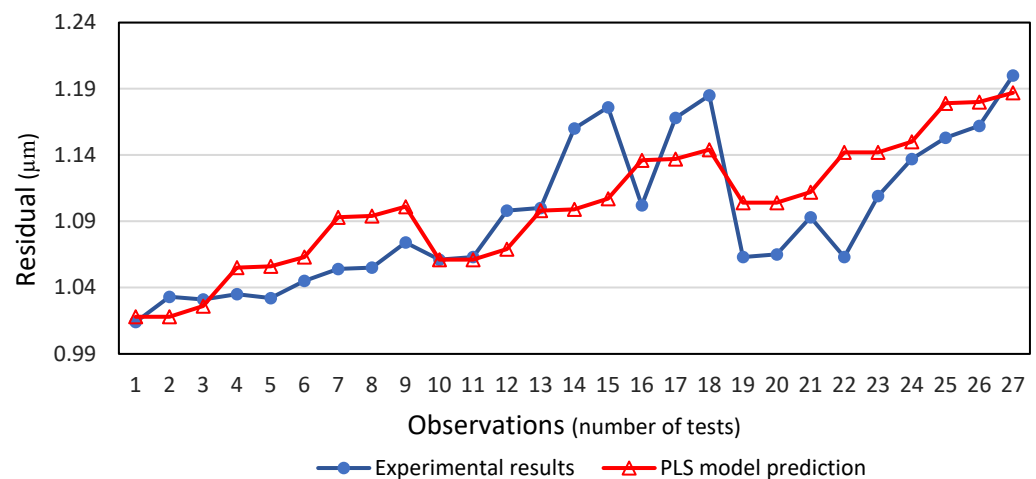

Figure 9. Comparison between experimental outputs and PLS regression prediction.

6.3. Effect of Process Variables on CFRP Delamination

Table 3 presents the experimental results and analysis of the delamination defect variance using three different tools. Table 5 provides a detailed analysis of the influence of various process parameters—namely feed rate, spindle speed, and tool number—on the delamination factor, using the signal-to-noise (S/N) ratio as a measure of performance. The S/N ratio, specifically calculated for the "smaller-the-better" criterion, indicates the robustness of the process against variability, with lower values suggesting better performance in minimizing delamination. Based on Figure 10, which displays the signal-to-noise (S/N) ratio plot for the delamination factor, and Table 5, it is clear that the best drilling input variables for reducing delamination were a spindle speed of 1000 rpm, a feed rate of 0.02 mm/rev, and the use of Tool (a), identified as a solid carbide drill with interior cooling holes. Additionally, Tool (a) consistently exhibited superior performance across all levels of feed rate and spindle speed, as indicated by the highest S/N ratios. This suggests that Tool (a) is more effective in achieving a stable and low delamination factor compared to Tools (b) and (c). Conversely, Tool (b) shows significantly lower S/N ratios, particularly at higher spindle speeds (2000 and 3000 RPM), indicating a higher susceptibility to delamination under these conditions.

Table 5. Main effect table (S/N ratio).

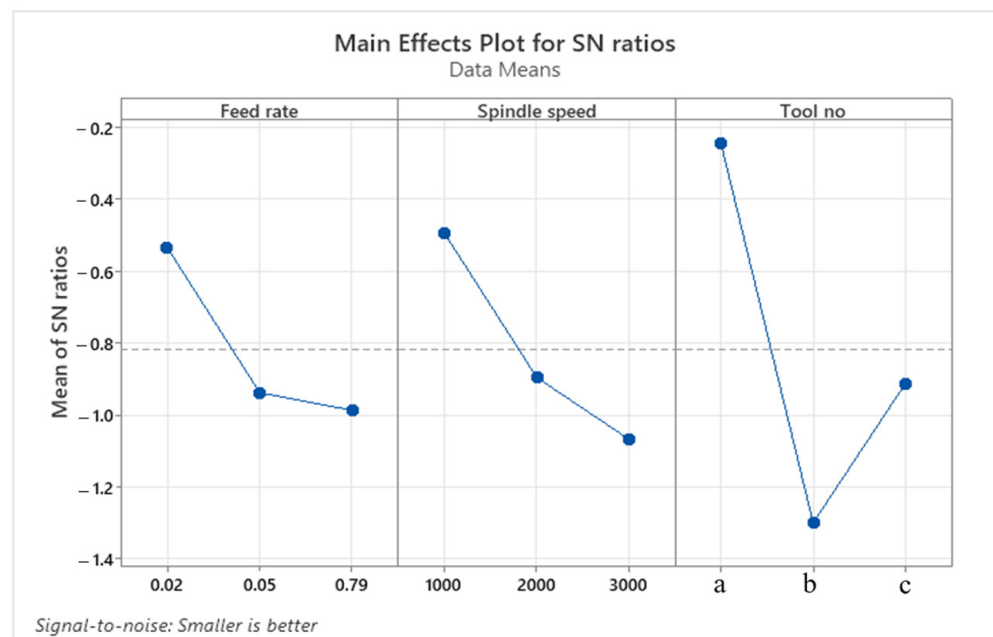| Feed Rate	Spindle Speed	Tool (a) (S/N Ratio)	Tool (b) (S/N Ratio)	Tool (c) (S/N Ratio)
0.02	1000	−0.121	−0.514	−0.531
0.02	2000	−0.299	−0.828	−0.531
0.02	3000	−0.206	−0.844	−0.930
0.05	1000	−0.366	−0.531	−0.547
0.05	2000	−0.274	−2.192	−0.899
0.05	3000	−0.240	−2.083	−1.304
0.79	1000	−0.265	−0.812	−0.772
0.79	2000	−0.214	−1.706	−1.115
0.79	3000	−0.231	−2.178	−1.584

Figure 10. S/N ratio plot for delamination factor.

To further our understanding, Figure 11 shows the influence of spindle speed and the feed rate on the delamination factor (Fd) across different tools, and contour plots were generated for each tool. The plots reveal distinct patterns for each tool, with Tool (a) showing a relatively stable delamination factor across varying feed rates and spindle speeds.

In contrast, Tool (b) exhibits a significant increase in the delamination factor at higher spindle speeds, particularly at lower feed rates. Tool (c) presents a more moderate rise in the delamination factor, but with less pronounced sensitivity to changes in operating conditions compared to Tool (b). These visualizations provide a clearer understanding of how each tool's performance is affected by the machining parameters, underscoring the importance of selecting the appropriate conditions to minimize delamination during the drilling process. The drill structure and cooling system shows statistical and physical significance in drilling CFRP plates. The analysis of variance results, presented in Table 6, indicates that variations primarily influence the delamination factor in tool structures. Specifically, the contribution rate of different tool structures (20.4%) outweighs the impact of spindle speed (9.4%) and the feed rate (9.1%). This suggests that delamination was primarily affected by the machining environment (friction effect), particularly the friction effect, as well as the tool structure.
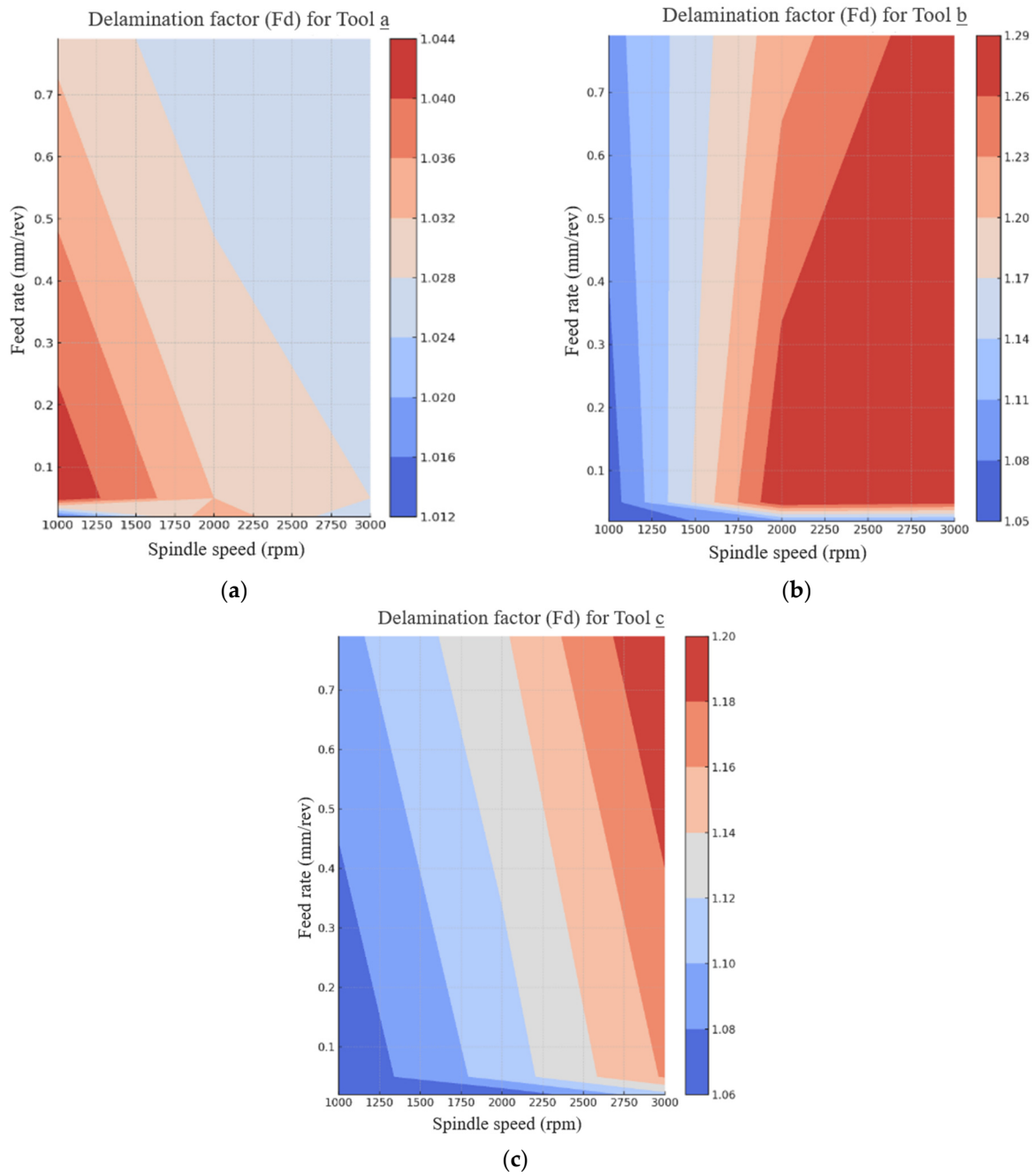
(**a**)

(**b**)

(**c**)

Figure 11. Contour plots showing the effect of spindle speed and feed rate on the delamination factor (Fd) for Tools (**a**) solid carbide drill, (**b**) end mill, and (**c**) step drill.

Table 6. Analysis of variance for delamination.

Source	DF	Seq SS	Adj SS	Adj MS	Contribution
Feed rate	2	1.111	1.111	0.5555	9.1%
Spindle speed	2	1.546	1.546	0.7732	9.4%
Tool no	2	5.101	5.101	2.5506	20.4%

7. Conclusions

In this research a partial least squares regression model was developed to predict the composite delamination coefficient during drilling operations on carbon fiber-reinforced plastic plates. The model utilized various descriptors to accurately predict the optimal

outcome of the drilling process, including the spindle speed, drill structure, and feed rate. In addition, the Taguchi method was employed to enhance the experimental design, ensuring a more efficient analysis of the machining parameters. The key findings and important points from this study are summarized as follows:

- The geometry of the tool and the cooling conditions, particularly friction, play a more significant role in influencing drilling outcomes than spindle speed and feed rate. These factors have been found to have the greatest impact on overall performance and quality during the drilling of the carbon fiber composite plates.
- The delamination defects observed in holes drilled using Tool (a) with an internal cooling system were reduced by 36.80% compared to the average results from the other tools tested. The internal cooling system effectively dissipates heat at the cutting zone, prolonging tool life. Additionally, it allows for the use of higher feed rates and spindle speeds, enhancing overall machining efficiency.
- The statistical model (PLS) achieved a Mean Squared Error (MSE) of 0.0045, indicating a very low prediction error and an accuracy of approximately 99.6%, which is essential for ensuring reliable predictions of delamination in the machining of the composite materials.
- The optimal drilling parameters to minimize delamination, as determined by Taguchi's method, include a spindle speed of 1000 rpm, a feed rate of 0.02 mm/rev, and the use of Tool (a), a solid carbide drill with internal cooling channels.

By integrating the Taguchi method with the partial least squares (PLS) approach, the study demonstrated that researchers could obtain a greater amount of quantitative data from fewer experiments. This combined approach optimized the experimental process while extracting more meaningful information from the results. The methodology could be extended to different machining processes to uncover statistical correlations between machining parameters and workpiece quality.

Author Contributions: Conceptualization, M.G.F. and H.B.; methodology, M.G.F. and H.B.; validation, M.G.F. and H.B; formal analysis, M.G.F. and H.B.; investigation, M.G.F. and H.B; resources, A.Z.; data curation, M.G.F. and H.B.; writing—original draft preparation, M.G.F. and A.A.; writing—review and editing, M.G.F. and A.A.; visualization, M.G.F., H.B. and A.A.; supervision, H.B. and A.Z.; project administration, H.B. and A.Z. All authors have read and agreed to the published version of the manuscript.

Data Availability Statement: Data are contained within the article.

Conflicts of Interest: The authors declare no conflicts of interest.

References

1. Xu, J.; Li, C.; Mi, S.; An, Q.; Chen, M. Study of drilling-induced defects for CFRP composites using new criteria. *Compos. Struct.* **2018**, *201*, 1076–1087. [CrossRef]
2. Rao, G.V.G.; Mahajan, P.; Bhatnagar, N. Micro-mechanical modeling of machining of FRP composites—Cutting force analysis. *Compos. Sci. Technol.* **2007**, *67*, 579–593. [CrossRef]
3. Xu, J.; Geier, N.; Shen, J.; Krishnaraj, V.; Samsudeensadham, S. A review on CFRP drilling: Fundamental mechanisms, damage issues, and approaches toward high-quality drilling. *J. Mater. Res. Technol.* **2023**, *24*, 9677–9707. [CrossRef]
4. Tsao, C.H.; Hocheng, H. Parametric study on thrust force of core drill. *J. Mater. Process. Technol.* **2007**, *192–193*, 37–40. [CrossRef]
5. Binali, R.; Da Silva, L.R.R.; Pimenov, D.Y.; Kuntoğlu, M.; Machado, A.R.; Linul, E. A Review on Progress Trends of Machining of Carbon Fiber reinforced Plastics. *J. Mater. Res. Technol.* **2024**, *33*, 4332–4359. [CrossRef]
6. Chen, R.; Li, S.; Zhou, Y.; Qiu, X.; Li, P.; Zhang, H.; Wang, Z. Damage formation and evolution mechanisms in drilling CFRP with prefabricated delamination defects: Simulation and experimentation. *J. Mater. Res. Technol.* **2023**, *26*, 6994–7011. [CrossRef]
7. Bhatnagar, N.; Nayak, D.; Singh, I.; Chouhan, H.; Mahajan, P. Determination of Machining-Induced Damage Characteristics of Fiber Reinforced Plastic Composite Laminates. *Mater. Manuf. Process.* **2004**, *19*, 1009–1023. [CrossRef]
8. Davim, J.P.; Reis, P.M. Drilling carbon fiber reinforced plastics manufactured by autoclave—Experimental and statistical study. *Mater. Eng.* **2003**, *24*, 315–324. [CrossRef]

9. Tsao, C.; Hocheng, H. A Review of Backup Mechanism for Reducing Delamination when Drilling Composite Laminates. *J. Res. Updates Polym. Sci.* **2016**, *5*, 97–107. [CrossRef]
10. Siddiquee, A.N.; Khan, Z.A.; Goel, P.; Kumar, M.; Agarwal, G.; Khan, N.Z. Optimization of Deep Drilling Process Parameters of AISI 321 Steel Using Taguchi Method. *Procedia Mater. Sci.* **2014**, *6*, 1217–1225. [CrossRef]
11. Fard, M.G.; Baseri, H.; Zolfaghari, A. Experimental investigation of the effective parameters and performance of different types of structural tools in drilling CFRP/AL alloy stacks. *J. Compos. Mater.* **2022**, *56*, 4461–4471. [CrossRef]
12. Zhang, Y.; Xu, X. Predicting the delamination factor in carbon fibre reinforced plastic composites during drilling through the Gaussian process regression. *J. Compos. Mater.* **2021**, *55*, 2061–2068. [CrossRef]
13. Zhang, Y.; Xu, X. Machine learning the magnetocaloric effect in manganites from compositions and structural parameters. *AIP Adv.* **2020**, *10*, 035220. [CrossRef]
14. Jong, W.R.; Huang, Y.M.; Lin, Y.Z.; Chen, S.C.; Chen, Y.W. Integrating Taguchi method and artificial neural network to explore machine learning of computer aided engineering. *J. Chin. Inst. Eng.* **2020**, *43*, 346–356. [CrossRef]
15. Zhang, Y.; Xu, X. Machine learning cutting force, surface roughness, and tool life in high-speed turning processes. *Manuf. Letters.* **2021**, *29*, 84–89. [CrossRef]
16. Zuperl, U.; Čuš, F. Tool cutting force modeling in ball-end milling using multilevel perceptron. *J. Mater. Process. Technol.* **2004**, *153–154*, 268–275. [CrossRef]
17. Aykut, Ş.; Gölcü, M.; Semiz, S.; Ergür, H.S. Modeling of cutting forces as function of cutting parameters for face milling of satellite 6 using an artificial neural network. *J. Mater. Process. Technol.* **2007**, *190*, 199–203. [CrossRef]
18. Zhang, Y.; Li, Y.; Zhang, J.; Pan, J.; Zhang, L.; Tan, F.; Wei, H.; Zhang, W. High-Temperature effect on the tensile mechanical properties of unidirectional carbon Fiber-Reinforced polymer plates. *Materials* **2021**, *14*, 7214. [CrossRef]
19. Geng, D.; Liu, Y.; Shao, Z.; Lu, Z.; Cai, J.; Li, X.; Jiang, X.; Zhang, D. Delamination formation, evaluation and suppression during drilling of composite laminates: A review. *Compos. Struct.* **2019**, *216*, 168–186. [CrossRef]
20. Sorrentino, L.; Turchetta, S.; Bellini, C. A new method to reduce delaminations during drilling of FRP laminates by feed rate control. *Compos. Struct.* **2018**, *186*, 154–164. [CrossRef]
21. Seif, A.; Fathy, A.; Megahed, A.A. Effect of drilling process parameters on bearing strength of glass fiber/aluminum mesh reinforced epoxy composites. *Sci. Rep.* **2023**, *13*, 12143. [CrossRef] [PubMed]
22. Liu, Y.; Li, Q.; Qi, Z.; Chen, W. Scale-span modelling of dynamic progressive failure in drilling CFRPs using a tapered drill-reamer. *Compos. Struct.* **2021**, *278*, 114710. [CrossRef]
23. Liu, Y.; Li, Q.; Qi, Z.; Chen, W. Defect suppression mechanism and experimental study on longitudinal torsional coupled rotary ultrasonic assisted drilling of CFRPs. *J. Manuf. Process.* **2021**, *70*, 177–192. [CrossRef]
24. Hocheng, H.; Tsao, C.C. Comprehensive analysis of delamination in drilling of composite materials with various drill bits. *J. Mater. Process. Technol.* **2003**, *140*, 335–339. [CrossRef]
25. Geier, N.; Xu, J.; Pereszlai, C.; Poór, D.I.; Davim, J.P. Drilling of carbon fibre reinforced polymer (CFRP) composites: Difficulties, challenges and expectations. *Procedia Manuf.* **2021**, *54*, 284–289. [CrossRef]
26. Tsao, C.; Hocheng, H. Evaluation of thrust force and surface roughness in drilling composite material using Taguchi analysis and neural network. *J. Mater. Process. Technol.* **2007**, *203*, 342–348. [CrossRef]